BACK PROPAGATION NEURAL NETWORK-BASED CUTTING FORCES PREDICTION IN DRY TURNING SKD11 STEEL OF HEAT TREATED WITH CBN INSERTS

DỰ ĐOÁN LỰC CẮT SỬ DỤNG MÔ HÌNH MẠNG LAN TRUYỀN NGƯỢC KHI TIỆN KHÔ THÉP SKD11 SAU NHIỆT LUYỆN VỚI DỤNG CỤ CẮT CBN

Hoang Thi Dieu[1,*], Tang Quoc Nam[1], Phung Van Binh[1]

DOI: https://doi.org/10.57001/huih5804.2023.221

ABSTRACT

Cutting force (CF) is one of the most important factors in improving machining efficiency. It directly affects the cutting tool life and the quality of the product. This paper presents the results of building a model to predict the value of the cutting force components using a back-propagation (BP) neural network when dry and hard turning SKD11 steel after heat treatment. The artificial neural network (ANN) training dataset is collected from 27 full dry turning experiments with CBN coated hard alloy cutting inserts and various cutting parameters including depth of cut, feed rate and cutting speed. The value of the cutting force components is measured by a specialized and modern force measuring device. The back-propagation neural network is established with many different structures to evaluate and select the most suitable structure. Indicators such as Coefficient of Regression (R2), Root Mean Square Error (RMSE) and Mean Absolute Percentage Error (MAPE) are used to assesment the quality of neural networks. The research results show that the generated neural network can effectively predict the value of the shear force components within the trained range. This result is the foundation for further research on vibration and tool wear as well as building a cutting force monitoring model during machining.

Keywords: *Hard turning, cutting forces, neural networks, Back-propagation, CBN inserts.*

TÓM TẮT

Lực cắt là một trong những yếu tố quan trọng nhất trong việc nâng cao hiệu suất gia công. Nó ảnh hưởng trực tiếp đến tuổi thọ của dụng cụ cắt và chất lượng sản phẩm. Bài báo này trình bày kết quả xây dựng mô hình dự đoán giá trị các thành phần lực cắt sử dụng mạng nơ ron lan truyền ngược khi tiện khô thép SKD11 sau nhiệt luyện. Bộ dữ liệu huấn luyện mạng nơ ron được thu thập từ 27 thực nghiệm toàn phần khi tiện khô với các mảnh cắt hợp kim cứng phủ CBN và các thông số cắt khác nhau bao gồm chiều sâu cắt, tốc độ chạy dao và vận tốc cắt. Giá trị các thành phần lực cắt được đo lường bằng thiết bị đo lực chuyên dụng và hiện đại. Mạng nơ ron lan truyền ngược được xây dựng với nhiều cấu trúc khác nhau để đánh giá và lựa chọn cấu trúc phù hợp nhất. Các chỉ số như hệ số hồi quy (Coefficient of Regression - R2), Root Mean Square Error - RMSE và sai số tuyệt đối phần trăm trung bình (Mean absolute percentage error - MAPE) được sử dụng để đánh giá chất lượng mạng nơ ron. Kết quả nghiên cứu cho thấy mạng nơ ron được ra có thể dự đoán hiệu quả giá trị các thành phần lực cắt trong phạm vi được đào tạo. Kết quả này là nền tảng để tiếp tục nghiên cứu về rung động và mòn dụng cụ cắt cũng như xây dựng mô hình giám sát lực cắt trong quá trình gia công.

Từ khóa: *Tiện cứng, lực cắt, mạng nơ-ron, lan truyền ngược, dụng cụ cắt CBN.*

[1]Faculty of Aerospace Engineering, Le Quy Don Technical University, Vietnam
[*]Email: hoangdieunute@gmail.com
Received: 05/8/2023
Revised: 05/10/2023
Accepted: 25/11/2023

1. INTRODUCTION

In recent decades, hard turning technology has been studied to replace grinding technologies in finishing hardening steel products [1-3]. During hard turning, thanks to the single-blade tool it is possible to precisely adjust the cutting angle and thus easily machine complex surfaces of the product. Compared with grinding, hard turning has many outstanding advantages in economic and ecological aspects [4]. The most significant advantage of hard turning is that it is possible to use one tool and still machine many different shaped parts by varying the toolpath. Meanwhile, if you want to sharpen other detailed shapes, you must fix the stone or change another stone. In particular, hard turning can process complex profiles that are difficult to achieve with grinding. Moreover, hard turning can also perform dry machining [5-7] without the use of cooling fluids, so it does not affect the environment and workers' health [8]. However, hard turning also requires a technological system with high rigidity and high accuracy [9].

In the machining process, many physical phenomena occur that affect the quality and productivity of machining vibration, friction,

P-ISSN 1859-3585 | E-ISSN 2615-9619

cutting force and tool wear [10, 11]. These factors all greatly affect product quality such as machining errors, mechanical properties and their ability to work. The causes for these phenomena to occur all stem from the selection and change of machining factors such as cutting parameters (cutting speed, depth of cut, feed rate), material of workpiece and tool, the rigidity of the technology system. Accordingly, the cutting force is one of the factors that change continuously throughout the machining process. Cutting forces are measured and analyzed in [12] during high-speed milling of aluminum alloys. The CF value is determined in the stable region and averaged. A mathematical model is built in [13] to predict the CF when microdril cutting. This factor prediction model was also developed in [14] in surface milling based on FEM and NURBS. The stochastic model of the CF is built and analyzed in [15] with the turning process through orthogonal CF measurements. The important results of this study show that the variance of the CF measurement signal is in the range of 4% - 9% of the mean value. The value of the marginal CF was investigated in [16] when milling the inclined plane with a cutter for hard alloy 55NiCrMoV6. The technique of signal processing to measure CF is described in detail in [17] when using a tunneling machine. The CF measurement and force spectrum analysis are described in [18] with milling through a PVDF thin film sensor. The CF prediction model including tool wear is also described in [19] during high-speed turning of Nimonic C263 superalloy.

The rapid development of computer science has made ANN a popular choice for building predictive models. The efficiency of applying ANN compared with other prediction methods is also compared as in [20, 21]. Different types of neural networks such as forward propagation [22, 23], convolutional network [24], back-propagation networks are widely used by scientists based on the superiority of and their effectiveness [25, 26]. The BP network is presented in [25] to build a predictive model of tool wear when turning H13 steel hardening. The predictive model of cutting heat, cutting force and tool wear is built based on the BP network in [26] during dry turning of Nimonic C263. Recently, convolutional networks (CNN) combined with image processing techniques have also been considered in some applied studies [24, 27-29], Fuzzy-ANN hybrid network [30, 31], deep learning network [32, 33].

This paper presents the results of establishing back propagation network to predict the value of cutting force components when turning hardening SKD11 steel without cooling after heat treatment. This BP network is built separately for each CF component with the Gradient Descent algorithm that continuously updates parameter sets of the BP networks. With various tests, a suitable BP networks structure to predict the value of each CF component has been determined. R^2, RMSE and MAPE criteria were used to evaluate the predictive quality of these BP networks. The research results are the foundation for building a cutting force monitoring and warning system as well as determining the cutting tool life under different machining conditions.

2. MATERIALS AND METHODS

2.1. Setup experimental system

The whole experiment was carried out on a HASS-ST10 lathe. Select SKD11 steel workpiece that has been heat treated to reach hardness 54÷56HRC, workpiece length is 300mm, and diameter is 30mm (Fig. 1). The chemical composition of the embryos is described in Table 1.

Table 1. Chemical composition SKD11 steel

Ingredients	C	Si	Mn	Cr	Ni	Mo	Va
%	1.45-1.65	≤ 0.4	≤ 0.35	11.0-12.5	0.25-0.4	0.4-0.6	0.15-0.3

For cutting tools, choose the CBN insert piece with symbol TNP-VNGA168408G2 (MB8025) of MITSUBISHI with specifications including IC = 9.525mm (Insert IC Size); LE = 16.606mm (Insert Cutting Edge Length); S = 4.76mm (Insert Thickness); RE = 0.8mm (Corner Radius); D1 = 3.81mm (Insert Hole Size).

Figure 1. Workpiece SKD11

The 9257BA-Kistler 3-component dynamometer is used to record the variation value of the CF in the three directions x, y, z respectively F_x, F_y, F_z. The instrument is supplied with the control box 5233A1, A/D converter, NI USB-6009 receiver (DAQ) and DASYLab 10.0 software. The tool wear value was determined after each machining interval with the help of an electron microscope UM012C. The experimental system is depicted in Figure 2.

The experiments were carried out with the set of technology regimes recommended by the cutting tool supplier and through a number of preliminary tests. The technical parameters are described in Table 2.

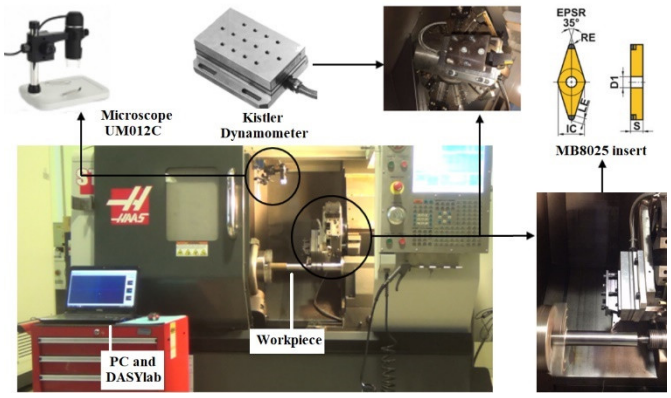

Figure 2. Machining and measuring systems

Table 2. Cutting parameters

Parameters	Level 1	Level 2	Level 3
V_c(mm/min)	80	125	170
s(mm/rev)	0.07	0.11	0.15
a_p(mm)	0.1	0.175	0.25

2.2. Measurement data processing

The measuring signal is the components of the shear force including F_x (axial force), F_y (radial force), F_z (tangent force). The total force F_{Total} is determined as follows

$$F_{Total} = \sqrt{F_x^2 + F_y^2 + F_z^2} \quad (1)$$

The components of the cutting force in turning and the location of the tool wear value are depicted as shown in Figures 3a and 3b.

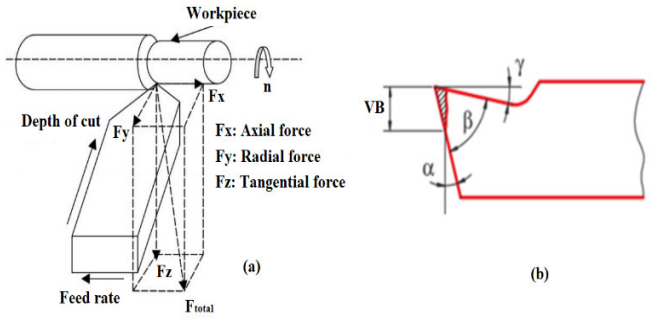

Figure 3. Cutting force components and tool wear measurement position

Figure 4 shows the interface when measuring and displaying the cutting force components. The CF value is presented in the form of a histogram.

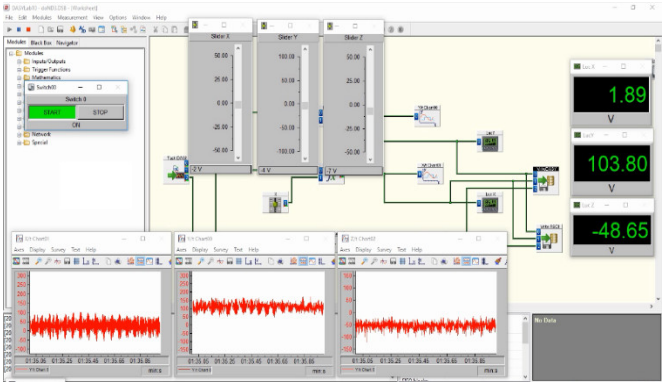

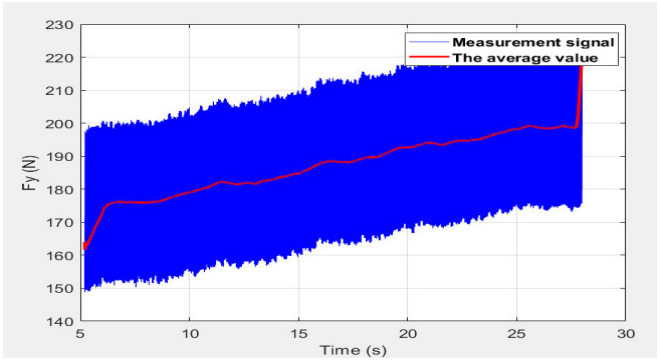

Figure 4. Measurement interface and signal processing results

The results after data processing and measurement are shown in Table 3. In which, F_{xa}, F_{ya} and F_{za} are the measured force values. The F_{xp}, F_{yp} and F_{zp} are the predicted force values from BP networks.

2.3. Back-propagation network structure and evaluation criteria

For BP networks, the adjustment of bias coefficients and weights takes place continuously during the training of the predictive model. These tuples are continuously updated through the loss function value control. The smaller the loss function value, the better the network quality. This means finding the minimum value of the loss function with the corresponding set of weights and bias coefficients. The algorithm commonly used in BP networks is Gradient Descent (GD). The most common approach is to start from a point that considering close to the solution of the problem or a random point on the loss function, and then use an iterative operation to progress to the desired point in descending order of the derivative value. It means until the derivative is close to 0. The parameters of the backpropagation network are updated as follows

$$w_{next} = w_{pre} - \alpha \frac{\partial J}{\partial w_{pre}}; b_{next} = b_{pre} - \alpha \frac{\partial J}{\partial b_{pre}} \quad (2)$$

In which, J is loss function; w_{pre} and w_{next} are the weights before and after the update, respectively; b_{pre} and b_{next} are the bias coefficients before and after the update; α is the learning rate. This factor is an important parameter used to control the number of iterations in the GD algorithm. When this parameter is small, the algorithm will need many iterations for the function to reach the minimum point. Conversely, if this parameter is large, the algorithm will need less iterations, but then the function may skip the minimum point and cannot converge. Predictive models based on ANN all have specific assessment criteria for model performance, accuracy and reliability. These indicators include R^2, RMSE and MAPE. The coefficient value R^2 represents the relationship between the predicted values and the random values. If the R^2 value approaches "1", the relationship is powerful. In contrast, if the value of R^2 approaches "0", the relationship is random. The larger the value of R^2 and the smaller the RMSE, the more reliable the model is.

Table 3. Actual and predicted values

Ex. No	a_p (mm)	V_c (m/min)	s (mm/rev)	Measured and predicted force values					
				F_{xa} (N)	F_{xp} (N)	F_{ya} (N)	F_{yp} (N)	F_{za} (N)	F_{zp} (N)
1	0.100	80	0.07	68.96	68.96	32.68	32.70	255.6	255.61
2	0.100	125	0.07	71.21	71.21	29.72	29.69	282.78	282.78
3	0.100	170	0.07	138.37	138.37	54.67	54.66	541.85	541.87
4	0.100	80	0.11	222.76	222.76	154.29	154.28	868.98	869.01
5	0.100	125	0.11	230.16	230.16	101.87	101.89	767.51	767.59
6	0.100	170	0.11	215.90	215.9	96.74	96.71	945.64	945.63
7	0.100	80	0.15	128.09	128.09	88.48	88.49	528.52	528.53
8	0.100	125	0.15	298.53	298.53	132.4	132.46	882.19	882.11
9	0.100	170	0.15	70.56	70.56	63.41	63.35	410.95	411.05
10	0.175	80	0.07	281.11	281.11	207.36	207.36	1117.5	1061.67
11	0.175	125	0.07	318.39	349.17	168.58	222.44	644.97	1132.75
12	0.175	170	0.07	149.16	223.58	115.65	115.67	564.73	564.76
13	0.175	80	0.11	243.57	243.56	99.23	99.25	755.16	755.17
14	0.175	125	0.11	295.93	295.93	168.95	168.88	1248.5	1248.42
15	0.175	170	0.11	65.66	290.2	28.16	28.25	257.05	257.09
16	0.175	80	0.15	380.06	380.06	258.45	258.40	1225.5	1225.45
17	0.175	125	0.15	222.74	222.74	162.88	162.94	804.77	804.98
18	0.175	170	0.15	285.96	285.96	120.74	120.63	880.56	880.48
19	0.250	80	0.07	333.51	333.51	271.32	271.30	1482.5	1482.49
20	0.175	125	0.07	379.96	349.17	222.43	222.44	1620.5	1132.75
21	0.250	170	0.07	305.98	305.98	236.9	233.02	1316.2	1316.25
22	0.250	80	0.11	58.99	58.99	7.99	8.00	228.17	228.23
23	0.250	125	0.11	341.00	400.81	142.14	185.11	720.64	980.75
24	0.250	125	0.11	460.63	400.81	228.08	185.11	1240.9	980.75
25	0.250	80	0.15	194.90	194.9	75.68	75.73	214.99	816.85
26	0.250	125	0.15	349.77	349.77	154.95	154.74	828.57	828.47
27	0.250	170	0.15	442.15	442.15	176.92	177.14	923.24	923.28

The expression defining R^2 is described as follows

$$R^2 = 1 - \left(\frac{\sum_{i=1}^{N} (y_{pi} - y_{ri})^2}{\sum_{i=1}^{N} y_{pi}^2} \right) \quad (3)$$

The expression of the RMSE is presented as follows

$$RMSE = \sqrt{\frac{1}{N} \sum_{i=1}^{N} (y_{pi} - y_{ri})^2} \quad (4)$$

The MAPE value entitles to estimate the deviation (in percentage) between the predicted value and the actual measured value. The expression for determining MAPE is defined as follows

$$MAPE = \frac{1}{N} \sum_{i=1}^{N} \left(\left| \frac{y_{pi} - y_{ri}}{y_{ri}} \right| \right) x100 \quad (5)$$

where, y_{pi} and y_{ri} are the predicted values from the model and the values measured in the i^{th} experiment, respectively. N is the number of experiments.

2.4. BP network training results and discussion

After many times of testing different network structures, it was found that the quality of ANN depends on many factors such as the number of input and output variables, the number of hidden layers and neurons in each hidden layer, the size of training dataset, the training algorithm, the proportion of data used in the network construction stages, and the nature of the actual model that needs to be predicted through the training dataset. Accordingly, in this

study, the BP network structure (3-10-30-1) corresponding to each cutting force component is described in detail as follows:

Number of input variables is 03 (corresponding to parameters a_p, V_c and s). The number of output variables is 01 (corresponding to each cutting force component). The number of hidden layers is 02. The number of hidden layer 1 neurons is 10 and the hidden layer 2 neurons is 30. The split ratio of training data is 80%, test data is 10% and validation is 10%. The data divided is random. The learning rate of the BP network is 0.01. The learning rate increase is 1.05. The learning rate reduction is 0.8. The training function is "traingdx". The transfer function is "logig". The number of iterations of training iterations is 5000. The network structure is depicted as shown in Figure 5. The loss function used in this case is RMSE.

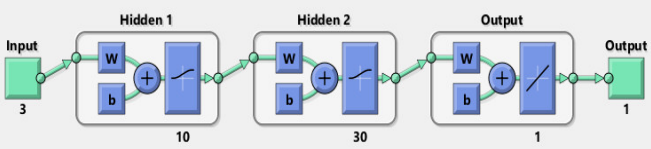

Figure 5. Network structure 3-10-30-1

The results of training the BP network for the cutting force component F_x are shown in Figure 6. Accordingly, the R^2 index in the training process reached over 0.98. The predictive value of CF on the entire learning data in Figure 7 shows that there is a large difference, especially in experiment 15. This directly affects the quality of the network.

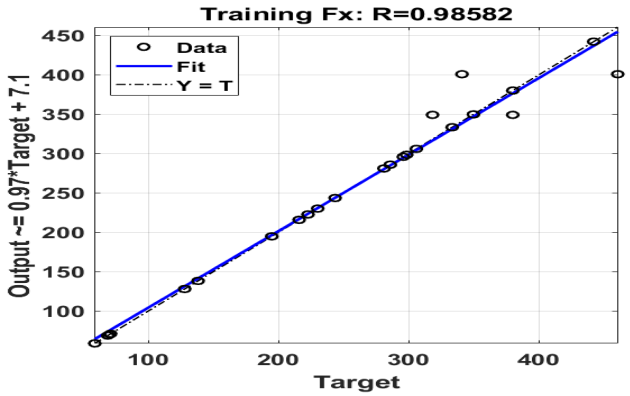

Figure 6. BP network training results for F_x

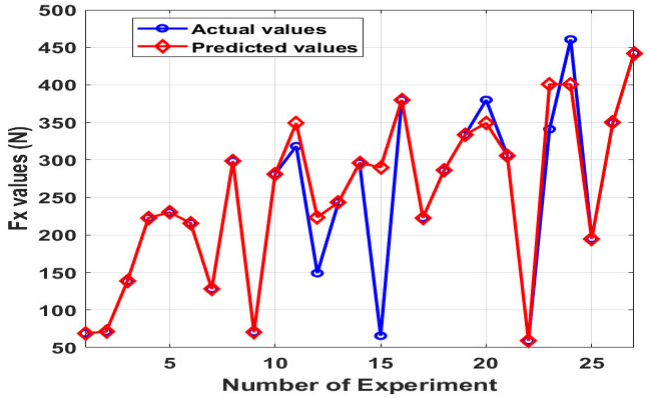

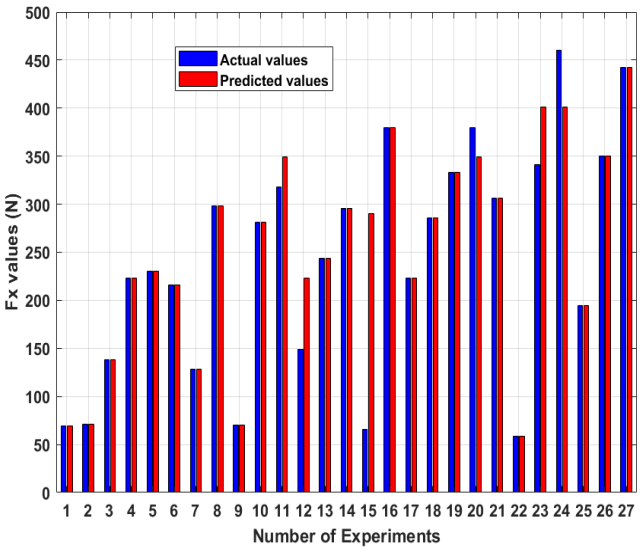

Figure 7. F_x prediction results

The training results of the BP network for the F_y in Figure 8 give good results with the R^2 value above 0.97. Figure 9 depicts the prediction results of the BP network on the entire learning data of the force component F_y. The difference between the actual values and the predicted values is not too large.

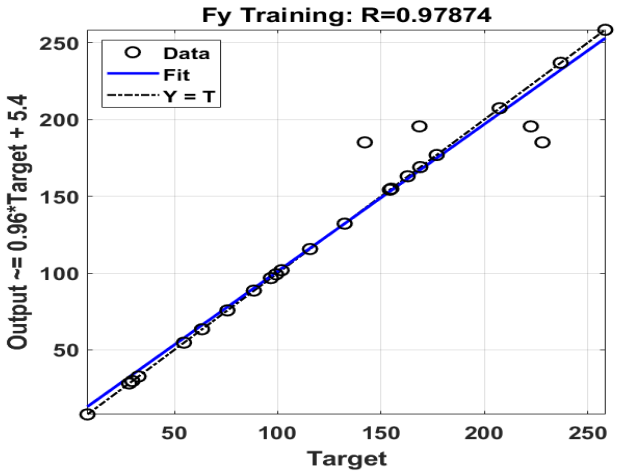

Figure 8. BP network training results for F_y

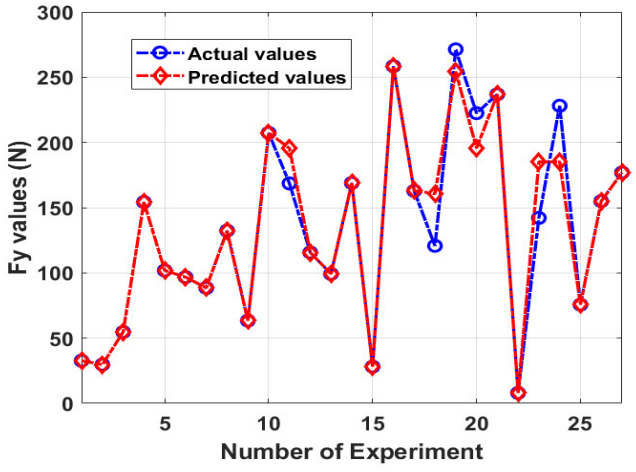

P-ISSN 1859-3585 | E-ISSN 2615-9619

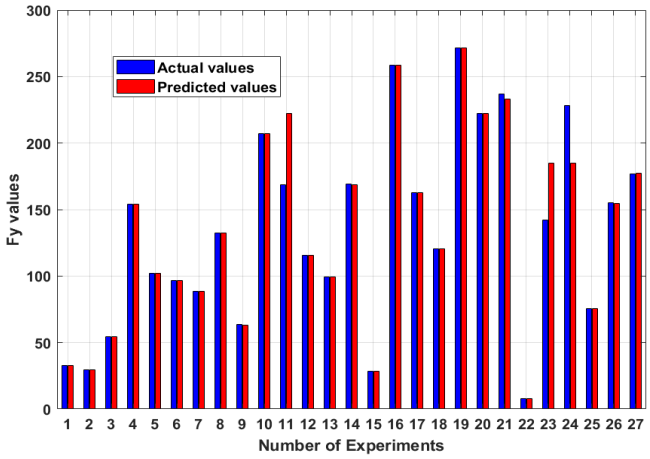

Figure 9. F_y prediction results

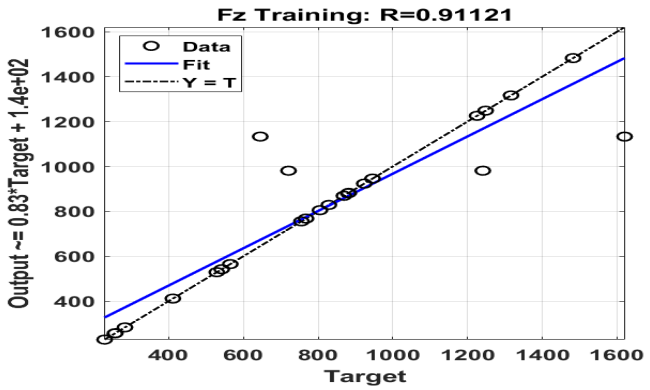

Figure 10. BP network training results for F_z

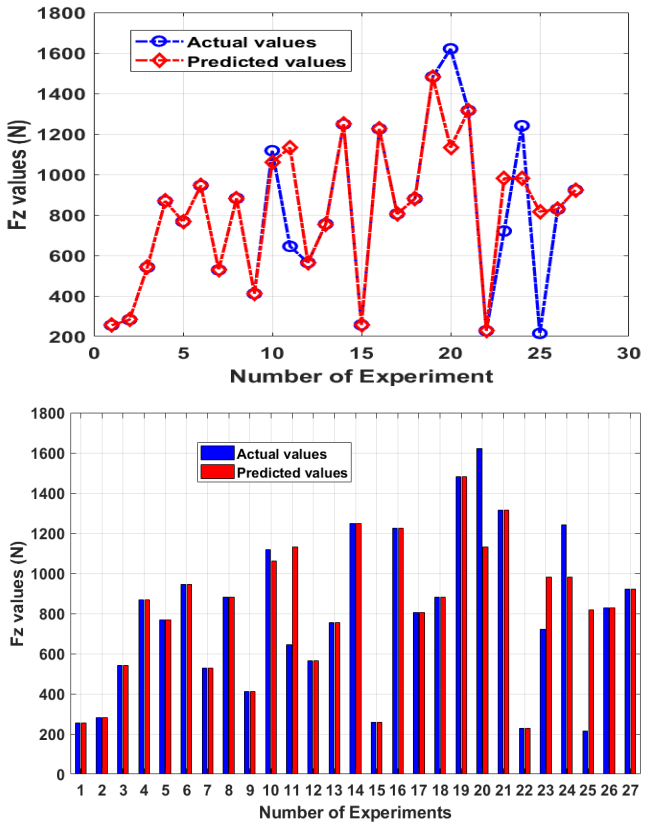

Figure 11. F_z prediction results

Figures 10 and 11 show the results of training the network and predicting the force component F_z value. The training result is only $R^2 = 0.91$. This is the lowest predicted result of the cutting force components. Accordingly, the prediction results on the entire learning data set also show many deviational values.

The criteria for evaluating the network quality on the whole prediction data are described in Table 4. Accordingly, the BP network predicts F_z for the lowest prediction quality while the BP network predicts F_y for the best quality ($R^2 = 0.988$; RMSE = 16.13; MAPE = 3.94).

Table 4. Values of network quality indicators

Criteria	BP-F_x	BP-F_y	BP-F_z
R^2	0.968	0.988	0.954
RMSE	49.07	16.13	190.17
MAPE	5.86	3.94	8.08

As can be seen, the results of estalishing BP networks to predict cutting force components clearly show some issues that need to be further addressed such as:

• The performance of the GD algorithm applied to the back-propagation network is highly dependent on the input data. Therefore, the processing of input data needs to be considered with a high degree of efficiency and reliability.

• It is easy to see that the back-propagation network with GD algorithm is quite sensitive to noisy data with a large difference in prediction values. Therefore, it is necessary to consider other solutions to improve the network training performance in particular and the prediction quality of the network in general.

• It is possible to consider building hybrid networks or combining BP networks with optimization algorithms to help train the network to achieve a global minimum for the loss function.

3. CONCLUSIONS

Predictive models of cutting force components have been successfully built based on backpropagation network structure with GD algorithm when turning hard and dry steel SKD11. The predictive performance of ANN networks is acceptable with the evaluation criteria R^2, RMSE and MAPE. The 3-10-30-1 network structure gives good prediction results with cutting force components F_y, F_x. The cutting force component F_z has a predicted result of over 91%. This reflects the reliability of the input data or the parameters of the ANN that have not reached the best value. Research results can also point out some points to pay attention to in the process of building the network as well as considering additional solutions to improve network quality.

REFERENCES

[1]. Özel T., Karpat Y., Figueira L., Davim J.P., 2007. *Modelling of surface finish and tool flank wear in turning of AISI D2 steel with ceramic wiper inserts*. Journal of materials processing technology, vol. 189, no. 1-3, pp. 192-198.

[2]. Niaki F.A., Michel M., Mears L., 2016. *State of health monitoring in machining: Extended Kalman filter for tool wear assessment in turning of IN718 hard-to-machine alloy*. Journal of Manufacturing Processes, vol. 24, pp. 361-369.

[3]. Orra K., Choudhury S.K., 2016. *Development of flank wear model of cutting tool by using adaptive feedback linear control system on machining AISI D2 steel and AISI 4340 steel*. Mechanical systems and signal processing, vol. 81, pp. 475-492.

[4]. Rech J., Moisan A., 2003. *Surface integrity in finish hard turning of case-hardened steels*. International Journal of Machine Tools and Manufacture, vol. 43, no. 5, pp. 543-550.

[5]. Sanchez Y., Trujillo F.J., Sevilla L., Marcos M., 2017. *Indirect monitoring method of tool wear using the analysis of cutting force during dry machining of Ti alloys.* Procedia Manufacturing, vol. 13, pp. 623-630.

[6]. Caggiano A., Napolitano F., Teti R., 2017. *Dry turning of Ti6Al4V: tool wear curve reconstruction based on cognitive sensor monitoring.* Procedia CIRP, vol. 62, pp. 209-214.

[7]. Reddy T.S., Banik T., Velagala R., Kashyap S., 2020. *A study and modeling of cutting forces in dry turning of heat treated AISI H13 tool steel with brazed tungsten carbide tip*. Materials Today: Proceedings, vol. 24, pp. 704-713.

[8]. Poulachon G., Bandyopadhyay B.P., Jawahir I.S., Pheulpin S., Seguin E., 2004. *Wear behavior of CBN tools while turning various hardened steels*. Wear, vol. 256, no. 3-4, pp. 302-310.

[9]. Diniz A.E., Ferreira J.R., 2003. *Influence of refrigeration/lubrication condition on SAE 52100 hardened steel turning at several cutting speeds*. International Journal of Machine Tools Manufacture, vol. 43, no. 3, pp. 317-326.

[10]. Lin Z.C., Chen D.Y, 1995. *A study of cutting with a CBN tool*. Journal of Materials Processing Technology, vol. 49, no. 1-2, pp. 149-164.

[11]. Lindvall R., Lenrick F., M'Saoubi R., Ståhl J-E., Bushlya V., 2021. *Performance and wear mechanisms of uncoated cemented carbide cutting tools in Ti6Al4V machining*. Wear, vol. 477, p. 203824.

[12]. Bolar G., Das A., Joshi S.N., 2018. *Measurement and analysis of cutting force and product surface quality during end-milling of thin-wall components*. Measurement, vol. 121, pp. 190-204.

[13]. Zhang H., Wang X., Pang S., 2014. *A mathematical modeling to predict the cutting forces in microdrilling*. Mathematical Problems in Engineering, vol. 2014.

[14]. Cai S., Yao B., Feng W., Cai Z., 2019. *An improved cutting force prediction model in the milling process with a multi-blade face milling cutter based on FEM and NURBS*. The International Journal of Advanced Manufacturing Technology, vol. 104, pp. 2487-2499.

[15]. Fodor G., Sykora H.T., Bachrathy D., 2020. *Stochastic modeling of the cutting force in turning processes*. The International Journal of Advanced Manufacturing Technology, vol. 111, pp. 213-226.

[16]. Wojciechowski S., Maruda R.W., Nieslony P., Krolczyk G.M., 2016. *Investigation on the edge forces in ball end milling of inclined surfaces*. International Journal of Mechanical Sciences, vol. 119, pp. 360-369.

[17]. Huang X., et al., 2018. *Cutting force measurement and analyses of shell cutters on a mixshield tunnelling machine.* Tunnelling Underground Space Technology, vol. 82, pp. 325-345.

[18]. Luo M., Chong Z., Liu D., 2018. *Cutting forces measurement for milling process by using working tables with integrated PVDF thin-film sensors*. Sensors, vol. 18, no. 11, p. 4031.

[19]. Amigo F.J., Urbikain G., de Lacalle L.N.L., Pereira O., Fernández-Lucio P., Fernández-Valdivielso A., 2023. *Prediction of cutting forces including tool wear in high-feed turning of Nimonic® C-263 superalloy: A geometric distortion-based model*. Measurement, vol. 211, p. 112580.

[20]. Özel T., Karpat Y., 2005. *Predictive modeling of surface roughness and tool wear in hard turning using regression and neural networks*. International journal of machine tools manufacture, vol. 45, no. 4-5, pp. 467-479.

[21]. Tangjitsitcharoen S., 2020. *Comparison of Neural Networks and Regression Analysis to Predict In-process Straightness in CNC Turning*. Procedia Manufacturing, vol. 51, pp. 222-227.

[22]. Liu Q., Altintas Y., 1999. *On-line monitoring of flank wear in turning with multilayered feed-forward neural network.* International Journal of Machine Tools Manufacture, vol. 39, no. 12, pp. 1945-1959.

[23]. Pant P., Chatterjee D., 2020. *Prediction of clad characteristics using ANN and combined PSO-ANN algorithms in laser metal deposition process.* Surfaces Interfaces, vol. 21, p. 100699.

[24]. García-Pérez A., et al., 2023. *CNN-based in situ tool wear detection: A study on model training and data augmentation in turning inserts*. Journal of Manufacturing Systems, vol. 68, pp. 85-98.

[25]. Özel T., Nadgir A., 2002. *Prediction of flank wear by using back propagation neural network modeling when cutting hardened H-13 steel with chamfered and honed CBN tools.* International Journal of Machine Tools Manufacture, vol. 42, no. 2, pp. 287-297.

[26]. Ayyaswamy J.P.K., Kulandaivel A., Ezilarasan C., Arunagiri A., Charles M., Kumar S.R., 2022. *Predictive model development in dry turning of Nimonic C263 by artificial neural networks*. Materials Today: Proceedings, vol. 59, pp. 1284-1290.

[27]. Mikołajczyk T., Nowicki K., Kłodowski A., Pimenov D.Y., 2017. *Neural network approach for automatic image analysis of cutting edge wear.* Mechanical Systems Signal Processing, vol. 88, pp. 100-110.

[28]. Mikołajczyk T., Nowicki K., Bustillo A., Pimenov D.Y., 2018. *Predicting tool life in turning operations using neural networks and image processing.* Mechanical systems signal processing, vol. 104, pp. 503-513.

[29]. Zhou X., et al., 2023. *Tool wear classification based on convolutional neural network and time series images during high precision turning of copper*. Wear, vol. 522, p. 204692.

[30]. Chungchoo C., Saini D., 2002. *On-line tool wear estimation in CNC turning operations using fuzzy neural network model.* International Journal of Machine Tools Manufacture, vol. 42, no. 1, pp. 29-40.

[31]. Naresh C., Bose P.S.C., Rao C.S., Selvaraj N., 2021. *Prediction of cutting force of AISI 304 stainless steel during laser-assisted turning process using ANFIS.* Materials Today: Proceedings, vol. 38, pp. 2366-2371.

[32]. Peng B., Bergs T., Schraknepper D., Klocke F., Döbbeler B., 2019. *A hybrid approach using machine learning to predict the cutting forces under consideration of the tool wear*. Procedia Cirp, vol. 82, pp. 302-307.

[33]. Misaka T., Herwan J., Ogura I., Furukawa Y., 2021. *Turning Process Monitoring with Deep Neural Network Trained by FEM Simulation.* Procedia CIRP, vol. 104, pp. 376-380.

THÔNG TIN TÁC GIẢ

Hoàng Thị Diệu, Tăng Quốc Nam, Phùng Văn Bình

Khoa Hàng không - Vũ trụ, Trường Đại học Kỹ thuật Lê Quý Đôn